ICSV13 - Vienna

The Thirteenth International Congress on Sound and Vibration

Vienna, Austria, July 2-6, 2006

STATE-SPACE MODELING OF THERMOACOUSTIC SYSTEMS FOR STABILITY ANALYSIS AND TIME DOMAIN SIMULATION

Christian Oliver Paschereit*, Jonas P. Moeck, and Mirko R. Bothien

Institut für Strömungsmechanik und Technische Akustik
Technische Universität Berlin
Müller-Breslau-Strasse 8
10623 Berlin, Germany
oliver.paschereit@tu-berlin.de

Abstract

In this work state-space methodology for modeling thermoacoustic systems is presented. Two applications are considered: time domain simulation of plane wave acoustic fields in combustor-like geometries and linear stability analysis. The stability analysis based on state-space models is applied to a model combustor and the results obtained are identical to those of an equivalent frequency domain calculation. In terms of computing time, the method proposed here is much faster and it is demonstrated that parametric studies to obtain stability maps can be conducted in a minimal amount of time. In addition to that, modeling and simulation results are compared to experimental data from an acoustic test rig and an atmospheric swirl stabilized burner. The approach is shown to produce accurate results.

INTRODUCTION

In order to lower NOx emissions, lean premixed combustion was introduced by the gas turbine industry. Combustion systems operating in this mode are, however, susceptible to self-excited oscillations arising due to the interaction of the unsteady heat-release and the acoustic field of the combustion chamber. This phenomenon, commonly referred to as thermoacoustic instability, implicates high amplitudes of oscillating pressure and heat release, thereby leading to structural wear and increased heat transfer to the combustor walls [1]. Predicting instabilities in gas turbine combustors is one of the crucial tasks for thermoacoustic system modeling. The traditional approach based on frequency response information of the individual system parts suffers from certain drawbacks. Finding the roots of the frequency domain dispersion relation which govern the stability of a thermoacoustic system is not a trivial task. Also, to solve for the systems eigenfrequencies and growth rates, a purely analytical description of the system must be available. Otherwise, graphical methods known from control theory [2, 3] can be used to determine system stability. In both cases, however, the methods are not practical for parametric studies, where stability is to be assessed for a large number of different parameter values.

Although CFD methods have proven to be able to accurately capture essential thermoacoustic interaction mechanisms [4], computing power and time demands are still very high. One possibility to decrease the computational costs is to couple a CFD solver to an acoustic network code (see e.g. [5]), where parts of the computational domain are represented by low-dimensional acoustic models.

The remainder of this paper firstly addresses the state-space approach to modeling of thermoacoustic systems. Subsequently, the methodology is used to represent the acoustic field in a combustor-like geometry in frequency and time domain. Stability analyses are applied to a simplified model system as well as to a real atmospheric swirl-stabilized combustor. In case of the model system, results are compared to a corresponding frequency domain calculation. For the test rig combustor, the effect of two different modes of fuel injection is incorporated in the model by means of their flame transfer functions. The results are compared to experimental data.

MODELING APPROACH

For frequencies below the cut-on frequency for the first non-planar mode the acoustic state at one location is completely defined by two variables. These variables can either be the acoustic pressure p' and velocity u' or the Riemann invariants f and g representing down- and upstream traveling waves, respectively. The primitive acoustic variables are related to the Riemann invariants by $p' = f + g$ and $u' = f - g$, where, as in the following, the acoustic pressure is scaled with the characteristic impedance of the medium.

Due to complex geometries and interaction mechanisms in technical systems, a comprehensive description of their acoustic field in all is very cumbersome [6]. Therefore, the system is split up into different subsystems. Each single subsystem is characterized by its transfer behavior relating the incoming Riemann invariants to the outgoing, i.e. in the scattering form. The complete system is reobtained by linking together the subsystems. This is done by connecting each subsystem's outputs to the inputs of its adjacent subsystems.

In Eq. (1) the state-space form of a generic acoustic element is given:

$$\begin{aligned} \dot{x} &= Ax + B \begin{bmatrix} f_u \\ g_d \end{bmatrix} \\ \begin{bmatrix} f_d \\ g_u \end{bmatrix} &= Cx + D \begin{bmatrix} f_u \\ g_d \end{bmatrix}, \end{aligned} \tag{1}$$

where subscripts u and d denote up- and downstream positions. A, B, C and D are time-invariant $N \times N$, $N \times 2$, $2 \times N$ and 2×2 matrices, respectively, and x is the N-dimensional state vector. The systems's termination, a reflection coefficient, for example, is a single input single output system and thus only a special form of Eq. (1).

Coupling of the subsystems' state-space representations results in one state-space formulation of the complete system. Interconnection of the subsystem models is not as straightforward as in frequency domain. In general, however, the interconnected system is obtained by matrix-algebraic manipulations of the subsystems' state-space matrices.

TIME DOMAIN SIMULATION OF PLANE WAVE ACOUSTICS

To validate the modular approach described in the precedent section, a time-domain simulation of an acoustic test rig is performed. Figure 1 shows a schematic overview of the facility split up into its subsystems. The up- and downstream ends are equipped with circumferentially mounted loudspeakers allowing for acoustic excitation of the rig. To determine the acoustic

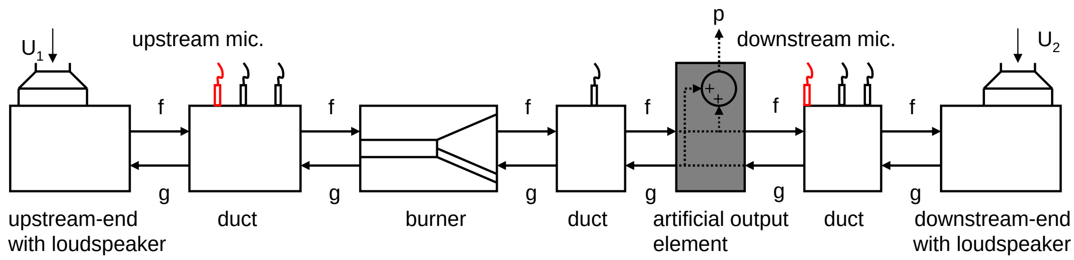

Figure 1: Schematic overview of the acoustic test facility with subsystem arrangement

field, it is instrumented with 1/4” condenser microphones. The ducts are 140 mm in diameter, thus only plane waves propagate in the frequency range considered (100 Hz−1 kHz).

The purpose of the validation is to show that the prediction of the acoustic field in the test facility matches the measured pressure fluctuations. The model’s inputs are the known speakers’ input voltages. The gray highlighted element in Fig. 1 is only a part of the model description (not a part of the real system). It writes out the predicted pressure fluctuation at the microphones’ positions.

Up- and downstream excitation is used to generate an acoustic field. Figures 2 and 3 show the transfer functions of the loudspeakers’ input voltages to the specified microphone positions (red highlighted microphones in Fig. 1). Note that the transfer function of the model (blue curve) is build up of the single transfer functions of each subsystem (i.e. terminations, ducts, burner, artificial output elements). Due to the modular setup, changes in geometry of the test rig can easily be implemented by changing or adding a subsystem to the model. Furthermore, it has the advantage that the determination of the subsystems’ transfer functions can be achieved in different ways. Here, the ducts and output elements are described analytically while the transfer functions for the burner and the end elements were obtained from experiments. By concatenation of the subsystem’s transfer functions a complete model with more than 200 states arose. Model reduction techniques were used to reduce the number of states to 70, exhibiting only slight deviations to the original transfer function. Despite some minor deviations, the model agrees almost perfectly to the measured transfer function (red curve).

With the reduced order model at hand pressure fluctuations at the two microphone positions were simulated in time-domain. The loudspeakers were driven with a signal composed of three sines at discrete frequencies. Furthermore, these sines were superposed with white noise, band-pass filtered between 100 Hz and 600 Hz. Figures 4 and 5 show the time traces

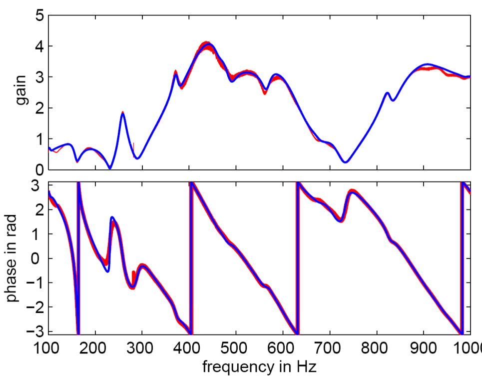

Figure 2: Gain and phase of measured (red) and modeled (blue) loudspeaker transfer function to upstream microphone

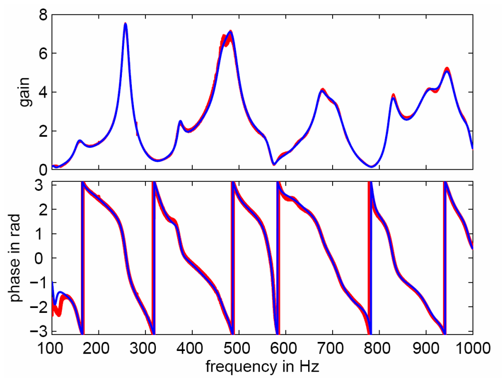

Figure 3: Gain and phase of measured (red) and modeled (blue) loudspeaker transfer function to downstream microphone

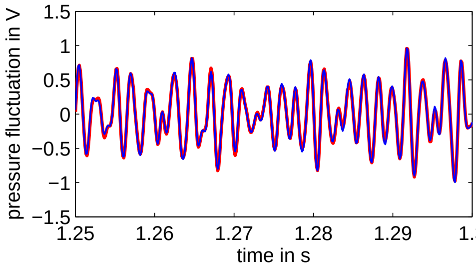

Figure 4: p' at upstream microphone; measured (red) and simulated (blue).

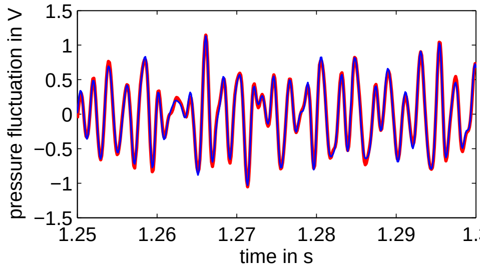

Figure 5: p' at downstream microphone; measured (red) and simulated (blue).

at up- and downstream positions, respectively. For both microphone positions the measured (red) and the predicted (blue) time responses show perfect agreement.

STABILITY ANALYSIS BASED ON STATE-SPACE MODELS

To assess the linear stability of a thermoacoustic network model based on state-space descriptions of the network components a procedure similar to the traditional frequency domain approach can be followed. Since the evolution of free oscillations has to be considered, no inputs will be present so that a homogeneous linear system $\dot{x} = Ax$ is obtained. Accordingly, if the dynamics matrix A has an eigenvalue with $\Re(s_n) > 0$ the internal system dynamics grow exponentially. Application of this procedure to thermoacoustic systems was proposed by Schuermans et. al. [6].

It is important to note here, that assessing system stability from a state-space description is almost trivial from a numerical point of view. Computing the eigenvalues of a given matrix can be done with standard routines. In particular no iterative or graphical methods are required as for example in [2, 3].

For the simplified case the upstream reflection coefficient is assigned a constant magnitude. The ducts are treated as lossless with plane wave propagation and including mean flow. For the burner transfer matrix the $L - \zeta$ model [7] is used. The linear flame response is represented by the flame model given in [8], where the flame transfer function is written as

$$F_Q = \frac{Q'}{u'}\frac{\bar{u}}{\bar{Q}} = \exp\left(-\mathrm{i}\omega\bar{\tau}_u - \frac{1}{2}\sigma_u^2\omega^2\right) - \exp\left(-\mathrm{i}\omega\bar{\tau}_\phi - \frac{1}{2}\sigma_\phi^2\omega^2\right). \tag{2}$$

Here, τ_u, σ_u, τ_ϕ and σ_ϕ are mean time-delays and variances of the distributions of fluctuating velocity and equivalence ratio. The corresponding transfer matrix for the acoustic variables is obtained by invoking the linearized Rankine-Hugoniot relations across the flame. The combustion chamber and the resonance tube are again modeled as lossless ducts. A long wave Levine-Schwinger boundary condition for an almost fully reflecting end describes the outlet.

To represent the infinite-dimensional terms (ducts and flame model) in a state-space model with finite dimension, rational approximations have to be made. The simple time-delays due to wave propagation can be brought to a rational form by making use of Padé approximants. The Gaussians in Eq. (2) are approximated using the one-over-polynomial approximation of order (6,4) given in [9].

The roots of the dispersion relation were determined using an iterative solver working on a uniformly distributed random field of intital guesses in a predefined rectangular subdomain of the ω-plane. A problem inherent to the frequency domain stability analysis is that due to the iterative nature of the solution process, it is in general not known if all relevant eigenvalues have been found. For the model system considered here, this problem can be overcome

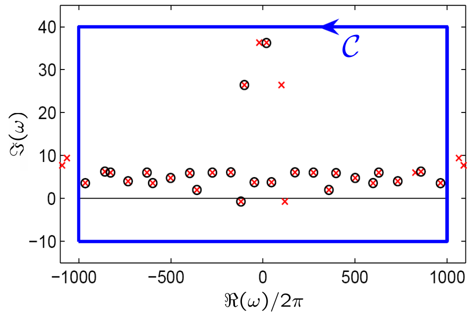

Figure 6: Eigenvalues of the state-space dynamics matrix of the interconnected system (×) and solutions of the frequency domain dispersion relation (∘); integration contour $\mathcal{C}$ used to evaluate the argument principle (⟵).

by making use of the argument principle (see e.g. [10]). For a function $\mathcal{D}(\omega)$ analytic on and inside a simple closed contour $\mathcal{C}$, the argument principle reads

$$\frac{1}{2\pi\mathrm{i}} \oint_{\mathcal{C}} \frac{\mathcal{D}'(\omega)}{\mathcal{D}(\omega)} \mathrm{d}\omega = \#\text{ of zeros inside } \mathcal{C}. \tag{3}$$

The individual elements' transfer matrices in the model problem considered are entire functions of ω. The determinant of the system matrix comprising all subsystem transfer matrices then obviously has the same property. Hence, Eq. (3) can be used to determine the number of complex eigenfrequencies in a given domain of the ω-plane. Even for the low complexity model system considered here, the expression of the determinant of the frequency domain system matrix is rather intricate. Therefore, obtaining the derivative of the dispersion relation with respect to ω as a closed form expression as required in Eq. (3) is not feasible. Instead of this, the derivative is computed numerically using finite differences.

Figure 6 shows the model system's eigenfrequencies for fixed parameters of the flame transfer function (Eq. (2)). The eigenvalues of the dynamics matrix A of the interconnected state-space model and iteratively determined solutions of the frequency domain dispersion relation are shown. Note that the eigenvalues of A have been rotated by -90° according to $\omega = -\mathrm{i}s$ so that $\Im(\omega) < 0$ indicates instability. The integration contour for the evaluation of the argument principle is also shown. As can be seen, the results from frequency domain and state-space calculation are virtually identical except for a few eigenvalues that are not found by the iterative solver. To ensure that the state-space approach indeed provides all eigenvalues in the domain considered, the contour integral in Eq. (3) is evaluated numerically from the frequency domain system matrix determinant. This calculation yields 30 up to an accuracy of 10^{-7} for the number of solutions of the dispersion relation inside $\mathcal{C}$ showing that the state-space model yields the right number of eigenvalues in the domain considered.

APPLICATION TO AN ATMOSPHERIC TEST RIG

The experimental results in this section were obtained from experiments conducted at an atmospheric test rig with a swirl stabilized burner. To investigate thermoacoustic instabilities a resonance tube could be attached to the combustor generating a high amplitude quarter wave mode instability at a frequency of around 100 Hz for certain operating conditions.

The state-space methodology for stability analysis is applied to investigate the impact of a redesigned fuel injection on thermoacoustic system stability. The fuel injection is redesigned as such that the majority of the fuel is directed to the outer flame region. This results in an enriched outer combustion zone (EOCZ) whereas the inner region is made leaner.

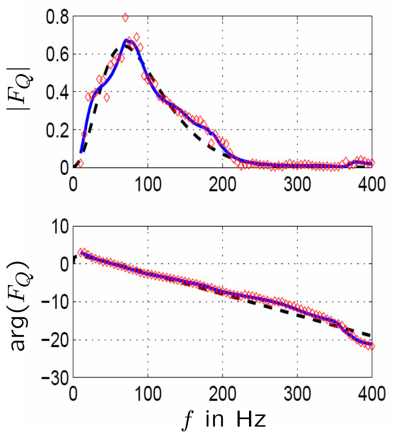

Figure 7: Flame transfer function for standard fuel injection; experimental (◇), Schuermans model (dashed line) and parametric state-space model (solid line).

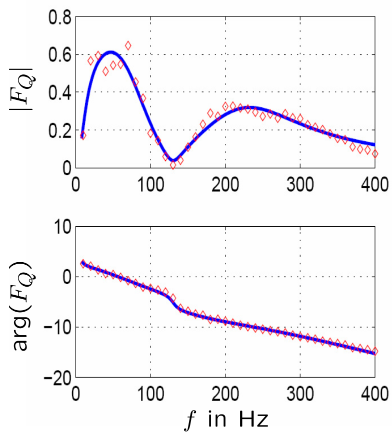

Figure 8: Flame transfer function for EOCZ injection; experimental data (◇) and parametric state-space model (solid line).

Flame transfer functions for both, the standard case and the EOCZ were determined experimentally. This was done via frequency response measurements of the OH-chemiluminescence of the flame and the plane wave acoustic field upstream of the burner. The latter was accomplished using the multi-microphone technique (see e.g. [8]). Excitation was provided by a woofer modulating the inlet air mass flow. State-space models accurately capturing the frequency response characteristics of the premixed flame were obtained using frequency domain system identification tools. Figures 7 and 8 show magnitude and phase of the flame transfer function for the standard case and for the EOCZ. The experimental data and the model results are shown. In case of the standard fuel injection, a fit of the analytical model of Schuermans et. al. [8] (see Eq. (2)) is also given.

Clearly, the EOCZ changes the flame response considerably. For the standard case, the response is essentially zero above 220 Hz. The transfer function phase exhibits a dominant time-lag. In magnitude and phase response it can be seen that the parametric model shows slightly better agreement than the analytic model of Schuermans et. al. [8] due to its higher flexibility. In case of the EOCZ the flame response has a zero at 130 Hz but attains a second local maximum in magnitude at around 220 Hz before it decays again. The flame transfer functions have been determined at the operating conditions, where stability is investigated. This was made possible by simply removing the resonance tube which always resulted in a stable system. Therefore, no scaling correlations for the flame transfer functions with equivalence ratio or power were neccessary as e.g. in [11].

In addition to the experimentally determined flame responses a parametric model of the upstream reflection coefficient was identified and included in the system model. This was considered neccessary since the upstream acoustic boundary condition was rather complex due to the preheater and air supply geometry. The complete model consisted of 11 elements and had a state dimension of 120.

Figure 9 shows the systems eigenfrequency distribution in the considered rectangular domain for the standard case and EOCZ injection. Obviously the model predicts that enriching the outer combustion zone has a distinct stabilizing effect on the combustor/resonance tube quarter wave mode. The initially unstable eigenvalue is moved across the real axis to the upper half-plane resulting in a stable system.

The stabilizing effect of the EOCZ could be verified in the experiment. Figure 10 shows pressure spectra recorded at the same operating conditions for the standard case and EOCZ

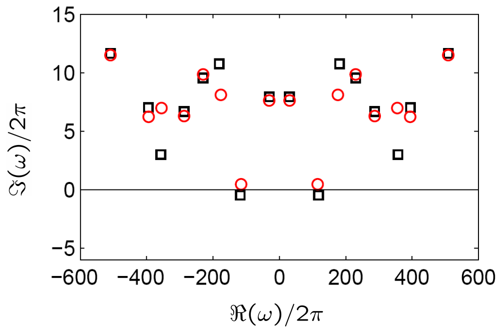

Figure 9: Eigenvalues of the system model, standard case(□) and EOCZ (○).

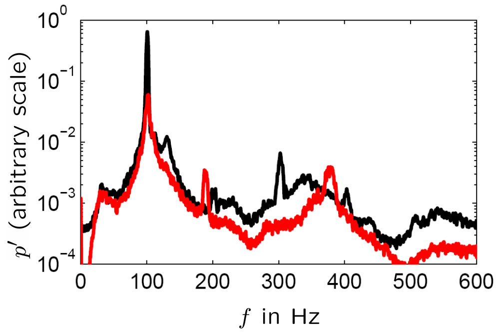

Figure 10: Combustor pressure spectra, standard case (black) and EOCZ (red).

injection. The pressure was measured directly at the flame with a 1/4" microphone in a probe holder built upon the semi-infinite tube principle. In the spectrum for the standard case, a dominant peak at 100 Hz corresponding to the quarter wave mode can be clearly seen. In contrast to that, the pressure spectrum from operation with EOCZ shows a significant reduction in the amplitude of the unstable mode (> 20 dB). In this case it is difficult to say if the system is actually stable as predicted by the model since the pressure amplitudes were still high. Yet, high pulsation amplitudes can be also exhibited by a stable lightly damped system driven by noise. However, the stabilizing effect of the EOCZ predicted by the model can be clearly seen in the experimental data. It should be mentioned, that EOCZ injection did not have a stabilizing effect at all operating conditions tested.

As a further application of the state-space approach for stability analysis the results of a parametric study are presented in Fig. 11. The colormap shows the growth rate $-\Im(\omega)$ of the least stable mode as a function of combustor length L and a shift in mean time-delay $\Delta\bar{\tau}$. The stability border, i.e. combinations of $(L, \Delta\bar{\tau})$ for which $\Im(\omega) = 0$ holds for the most unstable mode, is also shown in the plot. The shift in mean time-delay was connected in series with the measured flame transfer function (without EOCZ), so that

$$\tilde{F}_Q(\omega; \Delta\bar{\tau}) = F_Q(\omega)\mathrm{e}^{-\mathrm{i}\omega\Delta\bar{\tau}},$$

where F_Q is the measured flame transfer function and $\tilde{F}_Q$ is the one that is used in the parametric stability analysis. A change in power or equivalence ratio usually results in a modified time-delay of the flame response. From Fig. 11 it becomes clear that instability can only occur if the combustor length exceeds a certain value. In that case, the mean time-delay has to lie in a certain range for the system to be unstable.

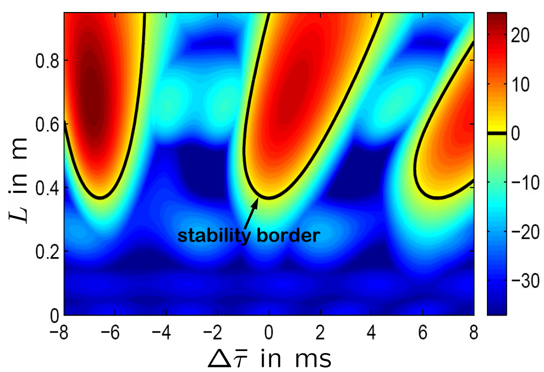

Figure 11: Growth rate $-\Im(\omega)$ of the least stable mode as a function of combustion chamber length L and mean time-delay shift $\Delta\bar{\tau}$. The thick black line denotes the stability border.

In contrast to the traditional frequency domain approach, generating stability maps using the state-space methodology is straightforward and time-efficient. For the results presented in Fig. 11 the stability problem has been solved 15'000 times in $(L, \Delta\bar{\tau})$ parameter-space in less than an hour. This would be impossible to accomplish by using graphical methods based on Bode or Nyquist diagrams as presented in [2, 3]. Even if analytical expressions for all transfer functions were available, generating a stability map based on solutions of the frequency domain dispersion relation would still be much more time-consuming.

SUMMARY

Modeling of (thermo-)acoustic systems in state-space by means of subsystem characterization was able to generate excellent results in both frequency and time domain simulation. The state-space representations of a simplified combustor model and an experimental combustion chamber were used for stability analysis. In comparison to the standard frequency domain approach, the state-space model produced exactly the same results with a fraction of computational effort. The impact of an enriched outer combustion zone on combustor stability was successfully captured by the model.

ACKNOWLEDGEMENTS

We thank A. Lacarelle for providing experimental combustor data with the EOCZ.

References

[1] Lieuwen, T. C., and Yang, V., eds., 2005. *Combustion Instabilities in Gas Turbine Engines*. AIAA, Inc.

[2] Sattelmayer, T., and Polifke, W., 2003. "Assessment of Methods for the Computation of the Linear Stability of Combustors". *Combust. Sci. Tech.,* **175**, pp. 453–476.

[3] Sattelmayer, T., and Polifke, W., 2003. "A Novel Method for the Computation of the Linear Stability of Combustors". *Combust. Sci. Tech.,* **175**, pp. 477–497.

[4] Roux, S., Lartigue, G., Poinsot, T., Meier, U., and Bérat, C., 2005. "Studies of mean and unsteady flow in a swirled combustor using experiments, acoustic analyis, and large eddy simulations". *Combustion and Flame,* **141**, pp. 40–54.

[5] Schuermans, B., Luebcke, H., Bajusz, D., and Flohr, P. "Thermoacoustic analysis of gas turbine combustion systems using unsteady CFD". ASME Paper 2005-GT-68393.

[6] Schuermans, B., Bellucci, V., and Paschereit, C. O. "Thermoacoustic modeling and control of multi burner combustion systems". ASME Paper 2003-GT-38688.

[7] Schuermans, B., Polifke, W., and Paschereit, C. O. "Modeling of transfer matrices of premixed flames and comparison to experimental results". ASME Paper 1999-GT-0132.

[8] Schuermans, B., Bellucci, V., Guethe, F., Meili, F., Flohr, P., and Paschereit, C. O. "A detailed analysis of thermoacoustic interaction mechanisms in a turbulent premixed flame". ASME Paper 2004-GT-53831.

[9] Nakamura, T. K., and Hoshino, M., 1998. "One-over-polynomial approximation for linear kinetic dispersion and its application to relativistic cyclotron resonance". *Phys. Plasmas,* **15**, pp. 3547–3551.

[10] Brown, J. W., and Churchill, R. V., 2004. *Complex Variables and Applications*, 7th ed. Mc Graw Hill.

[11] Kopitz, J., Huber, A., Sattelmayer, T., and Polifke, W. "Thermoacoustic stability analysis of an annular combustion chamber with acoustic low order modeling and validation against experiment". ASME Paper 2005-GT-68797.